

See discussions, stats, and author profiles for this publication at: <https://www.researchgate.net/publication/12131147>

# Secondary Ion Mass Spectrometry of Zeolite Materials: Observation of Abundant Aluminosilicate Oligomers Using an Ion Trap

ARTICLE *in* ANALYTICAL CHEMISTRY · FEBRUARY 2001

Impact Factor: 5.64 · DOI: 10.1021/ac000742a · Source: PubMed

---

CITATIONS

14

---

READS

27

6 AUTHORS, INCLUDING:



Gary S Groenewold

142 PUBLICATIONS 2,173 CITATIONS

SEE PROFILE



Anita K Gianotto

Idaho National Laboratory

30 PUBLICATIONS 466 CITATIONS

SEE PROFILE

# Secondary Ion Mass Spectrometry of Zeolite Materials: Observation of Abundant Aluminosilicate Oligomers Using an Ion Trap

Gary S. Groenewold,\* Glen F. Kessinger, Jill R. Scott, Anita K. Gianotto, Anthony D. Appelhans, and James E. Delmore

Idaho National Engineering and Environmental Laboratory, Idaho Falls, Idaho

Recep Avci

Image and Chemical Analysis Laboratory, Department of Physics, Montana State University, Bozeman, Montana

**Oligomeric oxyanions were observed in the secondary ion mass spectra (SIMS) of zeolite materials. The oxyanions have the general composition  $\text{Al}_m\text{Si}_n\text{O}_{2(m+n)}\text{H}_{(m-1)}^-$  ( $m + n = 2$  to 8) and are termed dehydrates. For a given mass, multiple elemental compositions are possible because (Al + H) is an isovalent and isobaric substitute for Si. Using 18 keV  $\text{Ga}^+$  as a projectile, oligomer abundances are low relative to the monomers. Oligomer abundance can be increased by using the polyatomic projectile  $\text{ReO}_4^-$  (~5 keV). Oligomer abundance can be further increased using an ion trap (IT-) SIMS; in this instrument, long ion lifetimes (tens of ms) and relatively high He pressure result in significant collisional stabilization and increased high-mass abundance. The dehydrates rapidly react with adventitious  $\text{H}_2\text{O}$  present in the IT-SIMS to form mono-, di-, and trihydrates. The rapidity of the reaction and comparison to aluminum oxyanion hydration suggest that  $\text{H}_2\text{O}$  adds to the aluminosilicate oxyanions in a dissociative fashion, forming covalently bound product ions. In addition to these findings, it was noted that production of abundant oligomeric aluminosilicates could be significantly increased by substituting the counteraction ( $\text{NH}_4^+$ ) with the larger alkali ions  $\text{Rb}^+$  and  $\text{Cs}^+$ . This constitutes a useful tactic for generating large aluminosilicate oligomers for surface characterization and ion–molecule reactivity studies.**

Aluminosilicate minerals play significant roles in geochemical processes in the subsurface and in the atmosphere.<sup>1,2,3</sup> Clay particulates, for example, consist of silicate minerals that normally have significant Al content. The fixed charge sites on the surface of clay and other minerals control adsorption and desorption processes that govern chemical mobility and modification in the environment.<sup>4–6</sup> Zeolites, a family of materials both naturally

occurring and man-made, include aluminosilicate phases that are used as catalysts and catalyst supports.<sup>7</sup> In addition, because the structural character of aluminosilicate zeolites includes defined cavities, they are important for industrial separations such as water removal. The significance of the aluminosilicate minerals has motivated considerable surface characterization research, but these efforts have been complicated because the commonly encountered minerals can be amorphous and highly heterogeneous. Characterization of environmental surfaces using static secondary ion mass spectrometry (SIMS) has been a focus in our laboratory, but research has emphasized adsorbate identification and quantification<sup>8</sup> and has largely ignored the underlying matrix.

SIMS has been used for characterization of alumina, silica, and clay surfaces to generate a combination of atomic<sup>9–12</sup> and molecular information.<sup>13,14</sup> Generally, the atomic information dominates the generated spectra, and the molecular ions, which contain chemical (as opposed to elemental) information, are difficult to observe. For example, a typical SIMS spectrum of silica is dominated by very abundant  $\text{O}^-$  and  $\text{OH}^-$  ions, and larger molecular species, such as  $\text{SiO}_2^-$ ,  $\text{SiO}_3^-$ , and  $\text{SiO}_3\text{H}^-$ , while usually observable, are dramatically less abundant. Using high sensitivity instruments, higher mass silicate<sup>15</sup> and aluminosilicate anions<sup>16</sup>

- (1) Buseck, P. R.; Posfai, M. *Proc. Natl. Acad. Sci., U.S.A.* **1999**, *96*, 3372–79.
- (2) Ravishankara, A. R. *Science* **1997**, *276*, 1058–65.
- (3) Bentz, J. W. G.; Goschnick, J.; Schuricht, J.; Ache, H. J. *Fresenius J. Anal. Chem.* **1995**, *353*, 559–64.
- (4) Koppelman, M. H.; Dillard, J. G. *ACS Symp. Ser.* **1975**, *18*, 186–201.
- (5) Zachara, J. M.; McKinley, J. P. *Aquat. Sci.* **1993**, *55*, 250–261.

- (6) Evans, L. J. *Environ. Sci. Technol.* **1989**, *23*, 1046–56.
- (7) Van Santen, R. A. *Theoretical Heterogeneous Catalysis*; World Scientific: River Edge, NJ, 1991.
- (8) For example, see Groenewold, G. S.; Appelhans, A. D.; Gresham, G. L.; Olson, J. E.; Jeffery, M.; Weibel, M. J. *Am. Soc. Mass Spectrom.* **2000**, *11*, 69–77.
- (9) Reed, S. J. B. *Mineral. Mag.* **1989**, *53*, 3–24.
- (10) MacRae, N. D.; Bottazzi, P.; Ottolini, L.; Vannucci, R. *Chem. Geol.* **1993**, *103*, 45–54.
- (11) Wang, Q. L.; Torrealba, M.; Gianetto, G.; Guisnet, M.; Perot, G.; Cahoreau, M.; Caisso, J. *Zeolites* **1990**, *10*, 703–6.
- (12) van Grieken, R.; Khoffer, C.; Wouters, L.; Artaxo, P. *Anal. Sci.* **1991**, *7* (Vol. 7 Suppl.), 1117–22.
- (13) Keyser, T. R.; Natusch, D. F. S.; Evans, C. A., Jr.; Linton, R. W. *Environ. Sci. Technol.* **1978**, *12*, 768–73.
- (14) Groenewold, G. S.; Gianotto, A. K.; Ingram, J. C.; Appelhans, A. D. *Curr. Top. Anal. Chem.* **1998**, *1*, 73–91.
- (15) Briggs, D.; Brown, A.; Vickerman, J. C. *Handbook of Static Secondary Ion Mass Spectrometry*; John Wiley & Sons: New York, 1989; p 150.
- (16) Vickerman, J. C.; Briggs, D.; Henderson, A. *The Static SIMS Library*; SurfaceSpectra Ltd.: Manchester, U.K., 1999, pp 1: 5.4B (Bentonite), 1: 5.7B (China Clay).

can be observed, but the abundance of these ions is usually so low that the application of high performance mass spectrometry methods such as accurate mass measurement, MS/MS, and ion–molecule reactions is impractical.

The low abundance of the larger mineral anions is a significant limitation, because they necessarily contain the richest chemical information that describes the surface and are the most interesting for conducting ion–molecule reactivity studies. Oligomeric silicates  $\text{Si}_x\text{O}_y\text{H}_z^-$  were observed by Bursey and Marbury, who were able to sputter species to  $x = 4$  from a basic sodium silicate solution.<sup>17</sup> Similar species were generated by three different groups using laser desorption.<sup>18–21</sup> More recently, Lafargue and co-workers were able to observe abundant silicate oxyanions using laser desorption Fourier transform mass spectrometry.<sup>22,23</sup> Silicate oligomers up to  $x = 11$  were generated, and they also noted relatively fast addition of gaseous  $\text{H}_2\text{O}$  to these species. The abundance of the oligomeric silicates was observed to peak about 10 ms after the laser pulse, which suggested that the ions were the result of ion–molecule reactions, but neither the monomeric anions ( $x = 1$ ) nor  $\text{OH}^-$  was identified as reactant ions. These earlier studies are related to the present research, in which we have analyzed aluminosilicate materials using a unique ion trap secondary ion mass spectrometer (IT-SIMS) instrument and have compared the results with more standard quadrupole and time-of-flight instruments. Because secondary ion lifetimes are long in the IT-SIMS and because the spectrometer vacuum is modest, ion–molecule reactions of the aluminosilicates with  $\text{H}_2\text{O}$  are observed. These water addition reactions appear to have dynamics that are similar to those of  $\text{Al}_2\text{O}_4\text{H}^- + \text{H}_2\text{O}$  that have been recently reported by our laboratory.<sup>24</sup>

## EXPERIMENTAL SECTION

**Sample Origin.** The Y-type zeolite sample that was used was designated CBV 712 and was acquired from Zeolyst International (Valley Forge, PA). It had a  $\text{SiO}_2/\text{Al}_2\text{O}_3$  ratio of 12 (Si/Al ratio 6.0) and the nominal counteraction as received was  $\text{NH}_4^+$ .

The  $\text{NH}_4^+$  was exchanged for the alkali cations by dropwise adding 15 mL of 0.34 M alkali nitrate solution to a ground zeolite/water slurry [ $\sim 1$  g zeolite in 30 mL distilled/deionized/demineralized water (resistivity,  $\sim 18$  M $\Omega$ )]. The slurry was stirred for 1–3 days, decanted, and washed three times with water. This process was repeated a total of three times, after which the exchanged zeolite was transferred as an aqueous slurry into a clean Petri dish, covered, and placed in a vacuum oven at  $\sim 373$  K (pumped by an oil-free pump to  $\sim 1$  mTorr) for approximately 12 h. Our experimental method is based on the method of Beck et al.,<sup>25</sup> the major differences being the concentrations of our

solutions and the number of times each zeolite sample was exchanged with the substituting counteraction. Unlike Beck et al., we found that repeated substitutions were necessary to remove most of the original cations. Mass spectral analysis of the substituted product was used to determine the efficacy of substitution (as measured by the ratio of the thermal ion currents of the substituted cation to the original cation), which was 15:1 or better after three substitutions. We suspect that the failure to get a higher ratio of substituted ion to original ion is based on the structure of the mordenite zeolite and the fact that some cation locations accessible to smaller ions are inaccessible to  $\text{Cs}^+$  because of its large size.

**Time-of-Flight SIMS.** Time-of-flight secondary ion mass spectrometry (TOF–SIMS) analyses were performed using a Phi–Evans triple focusing TOF–SIMS instrument (TRIFT),<sup>26,27</sup> located at the Image and Chemical Analysis Laboratory at Montana State University. In the present study, zeolite powder was pressed into indium foil and mounted in the sample holder of the instrument. The sample was then admitted to the source and analyzed at a base pressure of approximately  $5 \times 10^{-9}$  Torr. A  $120 \times 120$   $\mu\text{m}$  area containing the impressed powder was scatter-rastered using the primary ion beam in a pulsed fashion. The scatter raster samples the target surface in a random fashion and is used because it is easier to mitigate charge build-up, as compared to pattern rastering in which neighboring regions are sequentially interrogated. The instrument employs a microfocused  $\text{Ga}^+$  gun operated at  $\sim 1$  nA DC, which was pulsed at a repetition rate of 10 kHz. The temporal width of a single pulse was  $\sim 15$  ns. This information was used to calculate a flux density of  $6.5 \times 10^9$  ions  $\text{s}^{-1}\text{cm}^{-2}$ . Particles were typically analyzed for 5 min, and hence the total dose imparted to the samples was about  $2 \times 10^{12}$  ions  $\text{cm}^{-2}$ . The primary  $\text{Ga}^+$  impact energy was 18 keV. The instrument utilizes a secondary ion immersion lens, which extracts and transmits ions having a wide kinetic energy distribution ( $\Delta E \sim 200$  V) from the sample surface to the entrance slit of the first of three  $90^\circ$  spherical sector analyzers. Hence, the instrument can compensate for secondary ions having variable secondary ion kinetic energy and angular distribution, which are factors that can be pronounced for surfaces having irregular surface topography. The design of the TRIFT enables nearly 100% extraction efficiency with nearly zero background counts in all mass ranges.

The mass resolution ( $m/\Delta m$ ) of the TOF was compromised to some extent by the irregular surface topography. Resolution was approximately 1500, which easily permitted distinction of inorganic from organic ions, but made distinguishing between different inorganic combinations difficult or impossible.

**Quadrupole SIMS.** The quadrupole SIMS used in this study was a home-built instrument based on an Extrel (Pittsburgh, PA) triple quadrupole mass spectrometer with 16.8-mm rods and a mass range of 530 amu.<sup>28</sup> The instrument is equipped with a  $\text{ReO}_4^-$  primary ion gun that is based on a ceramic emitter design.<sup>29</sup> A

(17) Bursey, M. M.; Marbury, G. D. *J. Chem. Soc. Chem. Commun.* **1986**, 80–81.

(18) Michiels, E.; Celis, A.; Gijbels, R. *Int. J. Mass Spectrom. Ion Phys.* **1983**, 47, 23–26.

(19) De Waele, J. K.; Swenters, I. M.; Adams, F. C. *Spectrochim. Acta*, **1985**, 40B, 795–800.

(20) Denoyer, E.; Natusch, D. F. S.; Surkyn, P.; Adams, F. C. *Environ. Sci. Technol.* **1983**, 17, 457–62.

(21) De Waele, J. K.; Adams, F. C. *Scanning Microsc.* **1988**, 2, 209–28.

(22) Lafargue, P. E.; Gaumet, J.-J.; Muller, J. F.; Labrosse, A. *J. Mass Spectrom.* **1996**, 31, 623–32.

(23) Lafargue, P. E.; Gaumet, J. J.; Muller, J. F. *Chem. Phys. Lett.* **1998**, 288, 494–8.

(24) Scott, J. R.; Groenewold, G. S.; Gianotto, A. K.; Benson, M. T.; Wright, J. B. *J. Phys. Chem. A*, **2000**, 104, 7079–90.

(25) Beck, S. T.; Warner, D. W.; Garland, B. A.; Wells, F. V. *Rev. Sci. Instrum.* **1989**, 60, 2653–2656.

(26) Fister, T. F.; Strossman, G. S.; Willett, K. L.; Odom, R. W.; Linton, R. W. *Int. J. Mass Spectrom. Ion Proc.* **1995**, 14, 387.

(27) Schueler, B.; Sander, P.; Reed, D. A. *Vacuum* **1990**, 41, 1661–4.

(28) Groenewold, G. S.; Delmore, J. E.; Olson, J. E.; Appelhans, A. D.; Ingram, J. C.; Dahl, D. A. *Int. J. Mass Spectrom. Ion Proc.* **1997**, 163, 185–95.

(29) Beck, S. T.; Warner, D. W.; Garland, B. F.; Wells, F. W. *Rev. Sci. Instrum.* **1989**, 60, 2653.

Ba(ReO<sub>4</sub>)<sub>2</sub>/Eu<sub>2</sub>O<sub>3</sub> ceramic in a Re cup is heated to a temperature of approximately 1000°K, at which point the ceramic emits gaseous ReO<sub>4</sub><sup>−</sup> that is accelerated and focused on target. The gun was operated at an ion energy of 5.25 keV, with the primary ion current controlled at about 100 pA. The zeolite samples were attached to sample holders with dimensions of approximately 2 × 3 mm using double-sided tape (3M, St. Paul, MN). Most of the primary ion current was delivered onto this area. The flux density was, thus,  $\sim 1.0 \times 10^{10}$  ions cm<sup>−2</sup> s<sup>−1</sup>.

The secondary ion extraction lens was operated in a pulsed extraction mode,<sup>30</sup> which means that anions and cations are alternately extracted from the secondary ion source. The extraction time for each polarity was adjustable, and the ratio [cation extraction time/anion extraction time] used in the present experiments was 2.0. The actual time required for a single cation/anion extraction cycle was 26 ms, divided as follows: 13.3 ms cation extraction, 3 ms electronics settle time, 6.7 ms anion extraction time, and 3 ms electronics settle time. Because the primary ion beam is deflected off-target during the settle times, the fraction of time the beam was on-target was 0.77 in these experiments. The instrument was scanned from *m/z* 10 to *m/z* 499 in 190.7 s, and a typical acquisition was 2 scans. Hence, the dose was  $3.1 \times 10^{12}$  ions cm<sup>−2</sup>, which is substantially less than the static SIMS limit, or dose equivalent to the onset of surface damage observable in the SIMS spectrum.<sup>31</sup>

**IT-SIMS.** The IT-SIMS that was used in this study was constructed from a Finnigan ITMS instrument (Finnigan Corp., San Jose, CA).<sup>32</sup> The primary ion gun, ion trap, and direct insertion probe are mounted in a collinear fashion. Ion detection is accomplished using a conversion dynode and an electron multiplier, both of which are located off the instrument axis on the same side of the trap as the primary ion gun.

The primary bombarding particle utilized was ReO<sub>4</sub><sup>−</sup>,<sup>33</sup> (see above), accelerated to 4.6 keV and focused through an aperture in the ion trap end cap having a radius of 625 μm. The primary ion current was typically 100 picoamps, which together with the aperture area, can be used to calculate a flux density of  $5.1 \times 10^{10}$  ions cm<sup>−2</sup> sec<sup>−1</sup>. The irradiation period (ionization time) was typically 10–200 ms, and a typical analysis consisted of 50 scans; thus, the normal ion dose was  $0.26 \times 10^{11}$  to  $5.1 \times 10^{11}$  ions cm<sup>−2</sup>.

Upon entering the ion trap, the primary ion beam traverses the trap and exits through an orifice in the opposite end cap where it impacts the sample on the end of the direct insertion probe. The sample is located approximately 2 mm behind the end cap orifice. The secondary ions that were formed were focused into the trap using a compact electrostatic lens which is operated at +200 V when analyzing negative ions and is located between the target and the trap. Because the ion trap is a rf device, the instrument works in a de facto self-charge-stabilizing mode regarding surface charging.<sup>34</sup>

The primary ion beam impacts the sample continuously during the ionization period, during which time the secondary ions are

Table 1. Lower Mass Anions Observed in SIMS Spectra of Cs-zeolite and Most Probable Compositions

<i>m/z</i>	comp	<i>m/z</i>	comp	<i>m/z</i>	comp	<i>m/z</i>	comp
16	O <sup>−</sup>	35	<sup>35</sup> Cl <sup>−</sup>	59	AlO <sub>2</sub> <sup>−</sup>	77	SiO <sub>3</sub> H <sup>−</sup>
17	OH <sup>−</sup>	37	<sup>37</sup> Cl <sup>−</sup>	60	SiO <sub>2</sub> <sup>−</sup>	80	SO <sub>3</sub> <sup>−</sup>
25	C <sub>2</sub> H <sup>−</sup>	43	AlO <sup>−</sup>	61	SiO <sub>2</sub> H <sup>−</sup>	96	SO <sub>4</sub> <sup>−</sup>
32	O <sub>2</sub> <sup>−</sup>	45	HCO <sub>2</sub> <sup>−</sup>	62	NO <sub>3</sub> <sup>−</sup>	97	HSO <sub>4</sub> <sup>−</sup>
33	O <sub>2</sub> H <sup>−</sup>	46	NO <sub>2</sub> <sup>−</sup>	76	SiO <sub>3</sub> <sup>−</sup>	103	AlSiO <sub>3</sub> <sup>−</sup>

collected in the trap at a He pressure of  $3 \times 10^{-5}$  Torr. Once an adequate number of secondary ions have been accumulated in the trap (tens to hundreds of ms), the primary beam is electrostatically deflected, and the ions in the trap can then be scanned out for single stage MS analysis. Once the ions are scanned out, a mirror lens deflects them into an off-axis dynode/channelplate multiplier assembly. During ionization, the ion trap was operated at a low mass cutoff of 40 amu. Alternatively, a delay time may be inserted between ion bombardment and scan out; this enables ions formed from ion–molecule reactions to be identified.

## RESULTS AND DISCUSSION

**Analysis of Zeolites Using TOF–SIMS.** The primary emphasis of this research was the characterization of the higher mass oligomeric aluminosilicate oxyanions that are observed in the IT-SIMS analysis of zeolite materials. Initially, however, the zeolites were analyzed using a TOF–SIMS instrument, which is capable of much higher mass resolution, and is not susceptible to ion molecule reactions due to its high vacuum conditions, high ion velocity, and short residence time. The TOF–SIMS instrument used in this study utilized a 18 keV Ga<sup>+</sup> primary ion source. This projectile produces more abundant atomic secondary ions and is less sensitive to organic adsorbates than is the polyatomic ReO<sub>4</sub><sup>−</sup> projectile used in the IT-SIMS or the quadrupole SIMS. These attributes result in a much cleaner spectrum that in turn is more amenable to elemental analysis.

Qualitatively, the SIMS spectra of the Cs<sup>+</sup> zeolite were identical to the spectra of the other zeolites that were analyzed; however, because the oligomeric anion abundances for Cs<sup>+</sup> zeolite were somewhat greater (see below), it was used for ion identification and instrument comparison in this section. The most abundant ions in the TOF–SIMS spectrum of Cs<sup>+</sup> zeolite correspond to O<sup>−</sup> and OH<sup>−</sup> at *m/z* 16 and 17. Low abundance molecular ions were observed at higher masses that were more representative of the aluminosilicate matrix target (Figure 1). The mass resolution of the TOF–SIMS was approximately 1500 (*m/Δm*), which was lower than the manufacturer's performance specification as a result of irregular surface morphology. Nevertheless, it was possible to assign elemental compositions for ions <100 amu by limiting the composition search to those elements that were anticipated from the zeolite surface. In addition, compositions were excluded that would require hypovalent Si or Al ions, or numbers of H atoms that would require alane or silane structures.

Several ions at lower mass were derived from low levels of organic, nitrate, and sulfate contamination (Table 1). Contamination from organic acids is responsible for ions at *m/z* 45 and high-mass shoulders on *m/z* 43 (C<sub>2</sub>H<sub>3</sub>O<sup>−</sup>) and 59 (C<sub>2</sub>H<sub>3</sub>O<sub>2</sub><sup>−</sup>). Species that are detected at *m/z* 46 and 62 are consistent with the presence of nitrate and those at *m/z* 80, 96, and 97, with the presence of

(30) Appelhaus, A. D.; Dahl, D. A.; Delmore, J. E. *Anal. Chem.* **1990**, 62, 1679.

(31) Vickerman, J. C. *Analyst*, **1994**, 119, 513–523.

(32) Groenewold, G. S.; Appelhaus, A. D.; Ingram, J. C. *J. Am. Soc. Mass Spectrom.* **1998**, 9, 35–41.

(33) Delmore, J. E.; Appelhaus, A. D.; Peterson, E. S. *Int. J. Mass Spectrom. Ion Proc.* **1995**, 146/147, 15–20.

(34) Dahl, D. A.; Appelhaus, A. D. *Int. J. Mass Spectrom. Ion Proc.* **1998**, 178, 187–204.



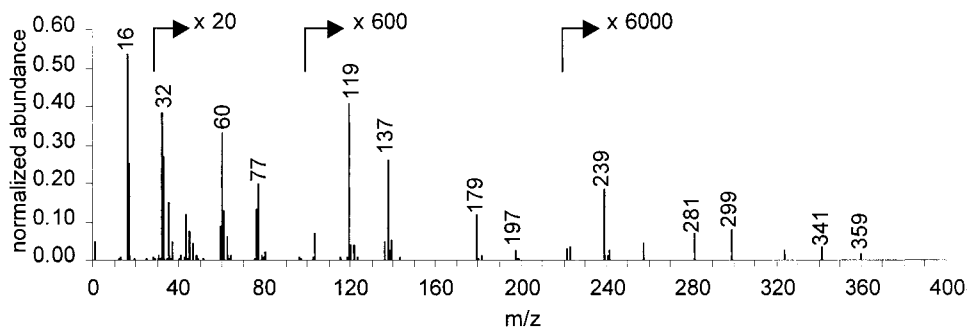


Figure 1. Anion TOF-SIMS spectrum of Cs zeolite (18 keV Ga<sup>+</sup> bombardment).

Table 2. Oligomeric Anion Series Observed in SIMS Spectra of Cs-zeolite and Most Probable Compositions

dehydrates $\text{Al}_m\text{Si}_n\text{O}_{2(m+n)}\text{H}_{(m-1)}^-$ ( $m+n$ ) = no.		monohydrates $\text{Al}_m\text{Si}_n\text{O}_{2(m+n)+1}\text{H}_{(m+1)}^-$ ( $m+n$ ) = no.		dihydrates $\text{Al}_m\text{Si}_n\text{O}_{2(m+n)+2}\text{H}_{(m+3)}^-$ ( $m+n$ ) = no.		trihydrates $\text{Al}_m\text{Si}_n\text{O}_{2(m+n)+3}\text{H}_{(m+5)}^-$ ( $m+n$ ) = no.		highly condensed $\text{Al}_m\text{Si}_n\text{O}_{2(m+n)-1}\text{H}_{m-3}^-$ ( $m+n$ ) = no.	
<i>m/z</i>		<i>m/z</i>		<i>m/z</i>		<i>m/z</i>		<i>m/z</i>	
119	2	137	2	155	2			221	4
179	3	197	3	215	3	233	3	281	5
239	4	257	4	275	4			341	6
299	5	317	5	335	5	353	5		
359	6	377	6	395	6	413	6		
		437	7	455	7	473	7		
				515	8				

sulfate. The remainder of the ions in the spectrum are derived from the aluminosilicate.

Molecular oxyanions containing aluminum are observed at *m/z* 43 and 59 ( $\text{AlO}^-$  and  $\text{AlO}_2^-$ ). At these low masses, the resolution is sufficient to permit composition assignment on the basis of accurate mass measurement. Ions at *m/z* 60, 61, 76, and 77 are interpreted in terms of the silicon bearing oxyanions  $\text{SiO}_2^-$ ,  $\text{SiO}_2\text{H}^-$ ,  $\text{SiO}_3^-$ , and  $\text{SiO}_3\text{H}^-$ , respectively, which can also be distinguished from Al-bearing possibilities on the basis of accurate mass measurement.

The lowest mass oligomeric oxyanion was observed at *m/z* 119 and could correspond to  $\text{AlSiO}_4^-$  and/or  $\text{Al}_2\text{O}_4\text{H}^-$ . Note that  $\text{Al} + \text{H}$  is both isobaric and isovalent with Si, and distinguishing Al + H-bearing compositions from Si-bearing compositions was problematic in this research. In the TOF-SIMS data, the accurate mass of the ion at *m/z* 119 was in better agreement with  $\text{AlSiO}_4^-$  (within 0.002 amu) than it was with  $\text{Al}_2\text{O}_4\text{H}^-$  (within 0.011 amu); however, the resolution of the instrument was not sufficient to permit unequivocal distinction of these ions, and hence, both may be present. Consideration of the isotopic signature of the ion was also ambiguous: Si has significant  $^{29}\text{Si}$  and  $^{30}\text{Si}$  isotopes, that would give rise to relatively abundant isotopic ions at *m/z* 120 and 121. These ions would not be abundant if the composition of *m/z* 119 were  $\text{Al}_2\text{O}_4\text{H}^-$ . However, the measured abundance of these ions was approximately twice what would be expected theoretically for  $\text{AlSiO}_4^-$ . Part of the ion abundance at *m/z* 120 and 121 was no doubt due to the presence of low-abundance  $\text{Si}_2\text{O}_4^-$ , and H-bearing anions. While we feel that  $\text{AlSiO}_4^-$  is the best fit for the mass spectrometric data and is consistent with the fact that the target is mostly Si, a contribution from  $\text{Al}_2\text{O}_4\text{H}^-$  cannot be excluded as a contributor to the signal at *m/z* 119. H/D exchange reactions were attempted to in order to distinguish between compositional possibilities, but contributions from background  $\text{H}_2\text{O}$  (from the zeolite and the IT vacuum atmosphere) could not be excluded.

*M/z* 119 is the lowest-mass constituent of an apparent oligomeric ion series that increments by 60 amu, to *m/z* 359 (Table

2). Above *m/z* 359, secondary ions were not observable in the TOF-SIMS spectrum. The 60-amu increment can be accounted for by either a  $\text{SiO}_2$  or a  $\text{AlO}_2\text{H}$  unit, although the  $\text{SiO}_2$  unit seems more likely in light of the composition of the zeolite ( $\text{Si}/\text{Al} = 6$ ). The ions can be described using the general composition  $\text{Al}_m\text{Si}_n\text{O}_{2(m+n)}\text{H}_{(m-1)}^-$  and are referred to as the dehydrates because the IT-SIMS experiments showed that  $\text{H}_2\text{O}$  readily adds them but cannot be eliminated from them (see below). Above *m/z* 119, the low abundance of the secondary ions and the mass resolution are inadequate for assigning elemental composition. Note, however, that these ions must contain at least one Al atom, because reasonable compositions of only Si, O, and H cannot be generated for these masses. This conclusion is also consistent with the notion that the presence of Al in a  $\text{SiO}_2$  matrix induces negative charge sites on the material surface, which may serve as precursors to the gas-phase secondary anions.<sup>5</sup>

A second oligomeric ion series in which the oligomeric species are separated by 60 amu is observed beginning at *m/z* 137. Possible compositions for *m/z* 137 may be generated by adding  $\text{H}_2\text{O}$  to those identified for *m/z* 119. In addition, a composition containing only Si ( $\text{Si}_2\text{O}_5\text{H}^-$ ) can account for *m/z* 137. The accurate mass measured for *m/z* 137 is in accord with either  $\text{Si}_2\text{O}_5\text{H}^-$  or  $\text{AlSiO}_5\text{H}_2^-$ .  $\text{Al}_2\text{O}_5\text{H}_3^-$  is in poorer agreement, but may account for a very minor component of the abundance at this mass. This composition is not favored because there is no reason to believe that the Al present in the zeolite is clustered. The general formula for this ion series is  $\text{Al}_m\text{Si}_n\text{O}_{2(m+n)+1}\text{H}_{(m+1)}^-$ ; the ions are referred to as the monohydrates because the IT-SIMS experiments showed that a significant fraction of these ions were formed by addition of  $\text{H}_2\text{O}$  to the dehydrates during storage in the ion trap.

Low-abundance ions at *m/z* 221, 281, and 341 are thought to constitute yet a third ion series, which we have designated as highly condensed. The composition for these ions can be written as  $\text{Al}_m\text{Si}_n\text{O}_{2(m+n)-1}\text{H}_{m-3}^-$ , and stable structures that can be deduced must contain significant unsaturation if the valence requirements of Al and Si are to be maintained. Ions having these masses and

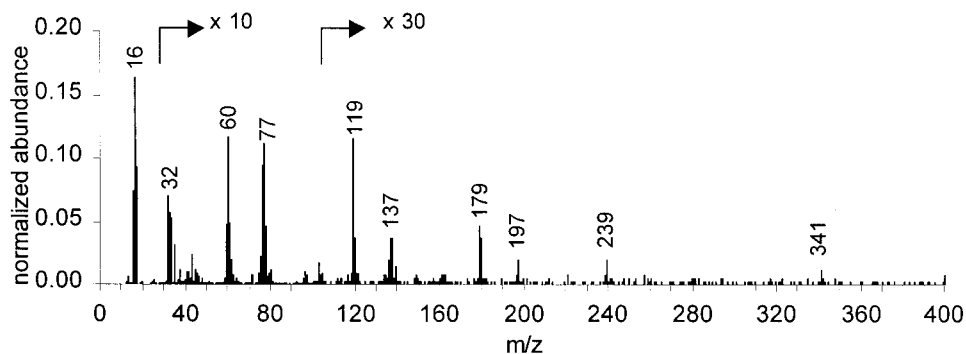


Figure 2. Anion quadrupole SIMS spectrum of Cs zeolite (5 keV  $\text{ReO}_4^-$  bombardment).

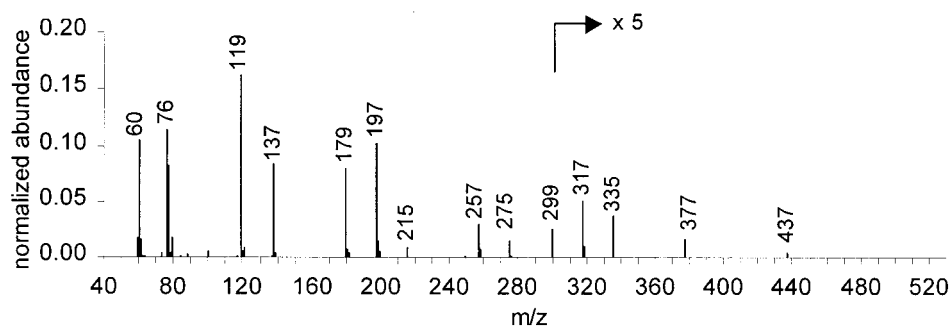


Figure 3. Anion IT-SIMS spectrum of cesium zeolite (4.5 keV  $\text{ReO}_4^-$  bombardment) acquired after 26-ms ion lifetime.

formulas can exist only if there are three or more Al atoms present (e.g., for  $m/z$  221,  $m$  can be either 3 or 4, but cannot be  $< 3$ ).

**Analysis of Zeolites Using Quadrupole SIMS.** The zeolite samples were analyzed using a quadrupole-based SIMS instrument that was equipped with a 5 keV  $\text{ReO}_4^-$  primary ion gun. This analysis was performed to facilitate comparison of the spectra acquired with the IT-SIMS with those acquired using the TOF-SIMS. The quadrupole SIMS is similar to the TOF-SIMS in that it operates under high vacuum conditions and ion lifetimes that are short in comparison to the ion trap. On the other hand, the quadrupole SIMS is similar to the IT-SIMS in that it employs a polyatomic projectile. The anion spectra of  $\text{Cs}^+$  zeolite acquired when using the quadrupole SIMS were qualitatively very similar to the TOF-SIMS data in that the ions that were observed were practically identical (Figure 2). A significant difference is that the normalized abundances of the molecular secondary ions in the quadrupole SIMS were greater than those in the TOF-SIMS. For example, the 119/60 abundance ratio is approximately  $10\times$  greater using the quadrupole, as compared to the TOF-SIMS. Several factors contribute to this observation, the foremost of which is that the polyatomic projectile  $\text{ReO}_4^-$  is more efficient at generating larger molecular secondary ions<sup>35</sup> than is the atomic projectile  $\text{Ga}^+$ . Conversely, the  $\text{Ga}^+$  primary generates augmented atomic and small molecular ions, as compared to the polyatomic. Above  $\sim m/z$  300, the trend of observing more abundant ions appears to be reversed in the quadrupole data; however, this is attributed to reduced high-mass transmission efficiency in the quadrupole, as compared to the TOF.

**Analysis of Zeolites Using IT-SIMS.** The IT-SIMS spectrum of  $\text{Cs}^+$  zeolite (Figure 3) does not include masses lower than  $m/z$  40, which was the low-mass cutoff for these experiments. Hence,

the abundance of the aluminosilicate anions cannot be compared to the abundance of  $\text{O}^-$  and  $\text{OH}^-$ , as in the case of the TOF and quadrupole-SIMS experiments. The low-mass cutoff was set at  $m/z$  40 because at lower values, the abundances of the higher-mass ions are significantly decreased as a result of inefficient trapping.

The molecular secondary ions at  $m/z$  60, 76, 77, 119, 137, and 179 are very similar to those observed in the TOF-SIMS and quadrupole SIMS spectra, with the notable exception that the oligomers are significantly more abundant in the IT than they are in either the quadrupole or the TOF. For example, the abundance ratio of [ $m/z$  119: $m/z$  60] is about 1.6 in the IT, as compared to 0.33 in the quadrupole and only 0.041 in the TOF. The augmented oligomer abundance is due to the effect of the polyatomic projectile (see above), the collisional stabilization that occurs in the ion trap after secondary ion sputtering,<sup>36–38</sup> and the fact that in the quadrupole, secondary ion transmission efficiency decreases with increasing mass. Collisional stabilization, which occurs throughout the ion trap, may be a significant factor: for macromolecules in ion traps, collisions with thermal He bath gas have been estimated to reduce the ion temperature from 450 to 300°K in 10 ms,<sup>39</sup> and similar behavior may well occur in the present experiments. Alternatively, abundant oligomeric secondary ions may be the result of gas-phase recombination reactions occurring in the IT-SIMS as a result of the long ion lifetimes in these experiments. If this process is contributing to the abundance of the oligomers, then it must be occurring in the region near the sample and not in the volume of the IT-SIMS where ions are trapped. This conclusion is derived from the observation that lengthening ion

(35) Groenewold, G. S.; Delmore, J. E.; Olson, J. E.; Appelhans, A. D.; Ingram, J. C.; Dahl, D. A. *Int. J. Mass Spectrom. Ion Proc.* **1997**, *163*, 1985–95.

(36) Castleman, A. W., Jr.; Keesee, R. B. *Chem. Rev.* **1986**, *86*, 589–618.

(37) Brodbelt, J. S. In *Practical Aspects of Ion Trap Mass Spectrometry*, March, R. E., Todd, J. F. J., Eds., CRC Press: New York, 1995; Vol. I pp 209–20.

(38) Lee, T. H.; Ervin, K. M. *J. Phys. Chem.* **1994**, *98*, 10023–31.

(39) Goeringer, D. E.; McLuckey, S. A. *Int. J. Mass Spectrom. Ion Proc.* **1998**, *177*, 163–74.

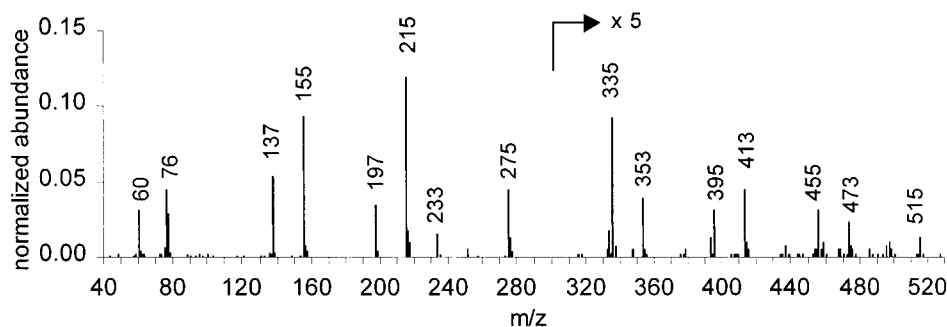


Figure 4. Anion IT-SIMS spectrum of cesium zeolite (4.5 keV  $\text{ReO}_4^-$  bombardment), acquired after 56-ms ion lifetime.

lifetime by the addition of a time period between ionization and detection does not increase the oligomeric abundances. Irrespective of the ion formation mechanisms involved, the result is that the abundances of all oligomeric anions are enhanced in the IT-SIMS analyses.

The second distinctive feature of the IT-SIMS spectrum in Figure 3 is the appearance of an additional ion series, which corresponds to the monohydrate series plus one additional  $\text{H}_2\text{O}$  molecule (Table 2). As indicated in the discussion of the TOF-SIMS data, different combinations of Al and Si are possible; however, in the IT-SIMS, the hydrated ion series predominantly arise through gas-phase ion-molecule reactions with adventitious  $\text{H}_2\text{O}$ , whereas in the TOF-SIMS, the ions in the hydrate series are sputtered from the surface because extensive ion-molecule reactions are unlikely. The adventitious  $\text{H}_2\text{O}$  is likely carried into the ion trap with the zeolite target, which is consistent with the adsorbent nature of the material. Typical background pressure in the IT-SIMS after operating the insertion lock was on the order of  $4 \times 10^{-7}$  Torr and slowly decreased as the zeolite was left in the vacuum chamber. Analyses of the vacuum atmosphere of our instruments using a residual gas analyzer (quadrupole MS) showed that the background was predominantly  $\text{H}_2\text{O}$ .

The reactions with adventitious  $\text{H}_2\text{O}$  occurred during the time between sputtering and scan out, which averaged 26 ms in this experiment. The ions in the new series are termed dihydrates, and have the general composition  $\text{Al}_m\text{Si}_n\text{O}_{2(m+n)+2}\text{H}_{(m+3)}^-$ . Careful examination of Figure 3 shows that as the size of the oligomer increases, the degree of hydration also increases. This is at least partly due to the fact that the higher mass oligomers spend a longer period of time in the IT-SIMS prior to ejection because the instrument scans from low to high mass and requires about 41 ms to go from  $m/z$  40 to 530. (For example, an ion at  $m/z$  40 would spend about 5.5 ms in the IT before being scanned out, as compared to an ion at  $m/z$  530, which would spend about 46.5 ms in the IT.) This observation emphasizes the impact of the long ion lifetimes in enabling the gaseous hydration reactions. Although a detailed evaluation of the kinetics of the hydration reactions is beyond the scope of this paper, a cursory look at the  $m/z$  119/137 ion ratio, the pressure, and the estimated ion lifetime suggests that the hydration reactions are fast: our data indicates that most of  $m/z$  137 is produced from 119, and if this is the case, a pseudo-first-order rate constant of  $1 \times 10^{-9} \text{ cm}^3\text{molecule}^{-1}\text{s}^{-1}$  can be calculated, which is close to what would be expected for a reaction occurring at the collision rate (average dipole orientation).<sup>40–42</sup>

The ion lifetime in the IT-SIMS was lengthened to an average of 56 ms in order to facilitate the observation of the hydrated ions (Figure 4). This decreased the abundance of the monohydrates and caused the dehydrates to disappear altogether. Conversely, the abundance of the dihydrates increased and yet another ion series appeared, which corresponded to the addition of a third  $\text{H}_2\text{O}$  molecule. The ions in this series are described by the general composition  $\text{Al}_m\text{Si}_n\text{O}_{2(m+n)+3}\text{H}_{(m+5)}^-$ , and are referred to as the trihydrates. The hydration reactions can be run toward completion by further increasing the ion lifetime; however, a point is reached at which the degree of hydration for the individual oligomers does not undergo appreciable change (see below). Interestingly, the degree of hydration was variable, depending on the oligomer being studied. Generally, under these conditions, negligible reactivity with  $\text{H}_2\text{O}$  was observed for the monomeric  $\text{SiO}_2^-$ ,  $\text{SiO}_3^-$ , and  $\text{SiO}_3\text{H}^-$ . The dimeric and tetrameric species ( $m+n=2, 4$ ) add up to two  $\text{H}_2\text{O}$  molecules, but evidently will not add a third. The trimer and penta- through octamers will add up to three  $\text{H}_2\text{O}$  molecules. Multiple molecular compositions and/or structures within a given oligomer no doubt result in variable degrees of hydration; for example, we have been unable to observe more than about 20% of the trimer as the trihydrate ( $m/z$  233), employing the longest ion lifetimes accessible using the IT-SIMS. This indicates that most of the trimer stops hydrating after the addition of two  $\text{H}_2\text{O}$  molecules, that is, the reaction of  $m/z$  215 plus  $\text{H}_2\text{O}$  will not proceed to completion, which is probably due to the presence of multiple compositions and/or structures at this mass. These observations point to the opportunity for more detailed hydration studies using the ion isolation-reaction approach.

**Influence of the Counteraction on the Production of the Aluminosilicate Oligomers.** A series of alkali cation-exchanged zeolites was analyzed during the course of the research, and it was found that substitution with  $\text{Rb}^+$  and  $\text{Cs}^+$  resulted in the enhanced emission of oligomeric aluminosilicates. Gnaser had observed similar behavior while bombarding  $\text{Cs}^+$ -doped surfaces.<sup>43</sup> This trend was identified by comparing the different alkali zeolites in terms of the abundances of the oligomeric anions (Figure 5, normalized to monomer abundances). For example, the abundance of the dimeric oligomers was 10 times greater from  $\text{Rb}^+$  than from  $\text{Na}^+$  zeolite.  $\text{NH}_4^+$  and  $\text{K}^+$  give intermediate responses, with  $\text{Cs}^+$  comparable to  $\text{Rb}^+$ . The data for the comparison presented in Figure 5 was generated using the IT-SIMS; a similar trend can be observed in the TOF-SIMS data, but the enhancements are less pronounced. We have not identified the reason

(40) Su, T.; Bowers, M. T. *Int. J. Mass Spectrom. Ion Phys.* **1973**, *12*, 347.

(41) Su, T.; Bowers, M. T. *J. Chem. Phys.* **1973**, *58*, 3027.

(42) Su, T.; Bowers, M. T. *Int. J. Mass Spectrom. Ion Phys.* **1975**, *17*, 211.

(43) Gnaser, H. *Int. J. Mass Spectrom. Ion Proc.* **1998**, *174*, 119–27.

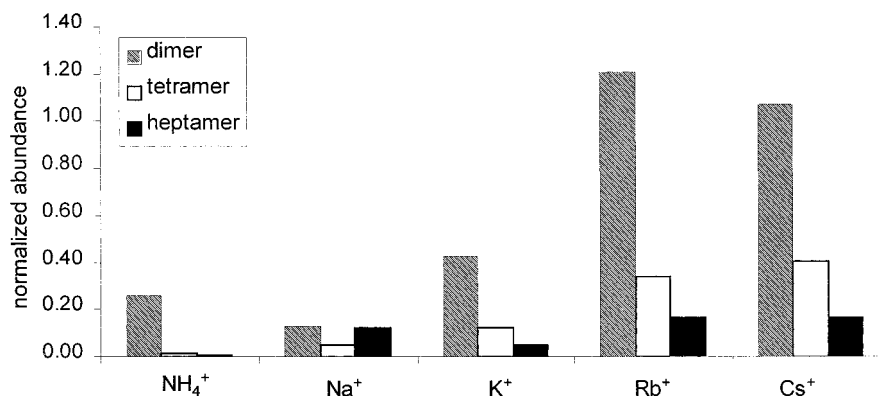


Figure 5. Oligomeric ion abundances for various alkali zeolites. Oligomer abundances are the sum of de-, mono-, di-, and trihydrates. Summed abundances were normalized relative to the sum of the monomeric abundances ( $m/z$  59, 60, 76, and 77). Data acquired using IT-SIMS.

for the enhancement, but have speculated that replacing the cations with Cs<sup>+</sup> or Rb<sup>+</sup> would reduce the surface work function: the work function of cesium oxide has been measured to be between 0.99 and 1.17 eV, which is much lower than the work function of either silica or alumina.<sup>44</sup> While Cs bonded to the zeolite oxygen atoms is different from pure Cs oxide, there is enough similarity to suggest that the Cs-substituted zeolites might have a similar low work function. A low value for the work function greatly expedites the energetic requirements for the release of a negative charge from a surface.

Alternatively, Cs<sup>+</sup> or Rb<sup>+</sup> substitution may facilitate emission of the oligomeric anions by more efficiently managing the surface charge of the zeolite under projectile bombardment. Surfaces under energetic particle bombardment generally emit secondary electrons in greater yield than ions. Because the dominant process is emission of electrons, the surface will tend to charge positively. A positive surface charge has a deleterious effect on the emission of secondary anions, particularly the larger molecular species,<sup>45</sup> which are emitted with lower kinetic energy than smaller species. Because the ionization potential decreases from Li through the alkali metals to Cs, the larger alkali cations are formed and emitted more readily, and this would serve to mitigate the build-up of positive charge. The alkali metal ions are readily observed when the instrument is operated in the positive ion mode.

## CONCLUSIONS

The present study resulted in the identification of oligomeric anion series, which is critical for identifying background ions observed in the negative SIMS spectra of naturally occurring minerals. In fact, the ion series can be observed in the SIMS spectra of sandy soils and clays,<sup>16,46</sup> albeit at much lower abundances. These abundances are so low as to be impractical to analyze directly from the naturally occurring minerals, hence the need for the current study. Because Al concentration is much lower in the soil samples than in the zeolites, the lower abundances observed in soils are in accord with the hypothesis that the presence of Al in the matrix facilitates observation of larger oligomers. Exact elemental compositions could not be unequiv-

cally established because (Al + H) and Si are isobaric and isovalent, and this represents a future characterization challenge. Multiple compositions at each oligomeric mass are likely.

In addition to dehydrated oligomers  $\text{Al}_m\text{Si}_n\text{O}_{2(m+n)}\text{H}_{(m-1)}^-$ , ions corresponding to mono-, di-, and trihydrates are observed which are the result of gas-phase ion–molecule reactions occurring with adventitious H<sub>2</sub>O present in the IT-SIMS. Recent ab initio modeling of aluminate monomers and dimers suggests that the addition of H<sub>2</sub>O molecules occurs in a dissociative manner, forming covalently bound adduct ions and not cluster ions.<sup>24</sup> The apparent rapid rate of H<sub>2</sub>O addition suggests that the aluminosilicates are behaving similarly. These observations suggest utilization of the IT-SIMS for the direct study of aluminosilicate oxyanions, which may be representative of fixed charge sites present on mineral surfaces. The approach would represent a facile means of examining the intrinsic reactivity of adsorption reactions that are important in atmospheric and subsurface geochemical processes.

The ability to conduct such ion–molecule reactivity investigations hinges on the production of abundant aluminosilicate anions, which can be augmented using Rb<sup>+</sup> or Cs<sup>+</sup> cation substitution. While the origins of the heavy-cation enhancement have not been defined, substitution represents a facile tactic for generating larger oligomeric anions directly from mineral surfaces. Because this research was completed, we have also had success enhancing oligomeric anions from alumina and silica surfaces by exchanging them with CsNO<sub>3</sub> solutions.

## ACKNOWLEDGMENT

The authors gratefully acknowledge the assistance of S. Greco, B. Marcus, and R. Quici of Zeolyst International (Valley Forge, PA), who provided technical information on Zeolyst zeolite products and arranged for us to receive complimentary zeolite samples that were used in this study, and the funding support of the Environmental Systems Research and Analysis Program, U.S. Department of Energy, Contract no. DE-AC-07-99ID13727 BBWI.

(44) Fomenko, G. S. *Handbook of Thermionic Properties*; Plenum Press: New York, 1966.

(45) Dahl, D. A.; Appelhans, A. D. *Int. J. Mass Spectrom. Ion Proc.* **1998**, *178*, 187–204.

(46) Groenewold, G. S.; Appelhans, A. D.; Gresham, G. L.; Olson, J. E.; Jeffery, M.; Wright, J. B. *Anal. Chem.* **1999**, *71*, 2318–23.

Received for review June 28, 2000. Accepted October 25, 2000.

AC000742A